ELSEVIER

www.elsevier.nl/locate/carres

Carbohydrate Research 324 (2000) 127–135

CARBOHYDRATE RESEARCH

The reduction of Cr^{VI} to Cr^{III} by the α and β anomers of D-glucose in dimethyl sulfoxide. A comparative kinetic and mechanistic study

Sandra Signorella, Rubén Lafarga, Verónica Daier, Luis F. Sala *

Departamento de Química, Facultad de Ciencias Bioquímicas y Farmacéuticas, UNR, Suipacha 531, 2000 Rosario, Argentina

Received 6 July 1999; accepted 18 October 1999

Abstract

The reduction of Cr^{VI} by α-D-glucose and β-D-glucose was studied in dimethyl sulfoxide in the presence of pyridinium *p*-toluensulfonate, a medium where mutarotation is slower than the redox reaction. The two anomers reduce Cr^{VI} by formation of an intermediate Cr^{VI} ester precursor of the slow redox step. The equilibrium constant for the formation of the intermediate chromic ester and the rate of the redox steps are different for each anomer. α-D-Glucose forms the Cr^{VI}–Glc ester with a higher equilibrium constant than β-D-glucose, but the electron transfer within this complex is slower than for the β anomer. The difference is attributed to the better chelating ability of the 1,2-*cis*-diolate moiety of the α anomer. The Cr^{V} species, generated in the reaction mixture, reacts with the two anomers at a rate comparable with that of Cr^{VI}. The EPR spectra show that the α anomer forms several linkage isomers of the five-coordinate Cr^{V} bis-chelate, while β-D-glucose affords a mixture of six-coordinate Cr^{V} mono-chelate and five-coordinate Cr^{V} bis-chelate. The conversion of the Cr^{V} mono- to bis-chelate is discussed in terms of the ability of the 1,2-*cis*- versus 1,2-*trans*-diolate moieties of the glucose anomers to bind Cr^{V}.

Keywords: Glucose anomers; Chromium; Redox mechanism

1. Introduction

Chromium is a well-known genotoxic and carcinogenic metal [1–3]. The biological reduction of Cr^{VI} to lower states has been observed with a wide variety of naturally occurring cellular reductants [4–8]. Ligands that possess two oxygen atoms able to form five-membered rings about the metal ion, such as 1,2-diols and α-hydroxy acids, are effective as non-enzymatic reductants and complexation agents towards hypervalent chromium and can stabilize the labile oxidation states of chromium [9–15]. For this reason, it is of interest to look at the ability of monosaccharides to reduce Cr^{VI} to Cr^{III}, a relevant aspect of the transport through soils of metal ions causing environmental pollution.

We have examined the reactions of Cr^{VI} with low-molecular-weight molecules [16–25]. Our previous studies on the reduction of Cr^{VI} by aldoses [16,26,27] and deoxyaldoses [16,19,21,26,27] afforded information on the relative abilities of these monosaccharides to reduce chromate, and the steric factors influencing the rate of oxidation of monosaccha-

* Corresponding author. Fax: +54-341-435-0214.
E-mail address: inquibir@satlink.com (L.F. Sala)

0008-6215/00/$ - see front matter
PII: S0008-6215(99)00282-7

rides by Cr^{VI} and by the intermediate Cr^{V} formed during the reaction course [27,28].

For all the aldoses studied, the C-1–OH hemiacetalic function reacts faster than the primary or any of the secondary alcoholic groups, and the aldonic acid (and/or the corresponding lactone) is the only reaction product when a ten-fold or higher aldose to Cr^{VI} ratio is used. An important point to be addressed in the chromic oxidation of these monosaccharides is the reactivity of the individual anomers. Under the acid conditions used in all the previous studies, the α and β anomers of the sugars equilibrate much faster than they react with Cr^{VI}, and so all of the reported results refer to the rates of chromic oxidation of equilibrium solutions of the sugars. In this work, we evaluate the Cr^{VI} oxidation rates of the individual anomers of D-glucose (Glc) in a medium where the mutarotation of the sugar is slower than the electron-transfer reaction. This study provides, for the first time, information on the relative abilities of the α and β anomers to reduce Cr^{VI} to Cr^{III}.

2. Experimental

Materials.—Pure α-D-glucose ($[\alpha]_D^{20} + 110°$ (*c* 5, water); mp 145.5 °C) and β-D-glucose ($[\alpha]_D^{20} + 18.9°$ (*c* 5, water); mp 149 °C) were prepared from pure D-glucose according to the method described by Hudson and Dale [29]. Water was purified by deionization, followed by double distillation from a solution of potassium permanganate. Dimethyl sulfoxide (Me_2SO) was purified before use [30]. $Na[Cr(O)(ehba)_2]\cdot H_2O$ was synthesized from 2-ethyl-2-hydroxybutanoic acid (Aldrich grade) and sodium dichromate (E. Merck) in acetone (E. Merck, A. R. grade) according to the literature method [31]. Pyridinium *p*-toluenesulfonate (PPTS) (mp = 119 ± 1 °C) was synthesized according to a previously described method [32].

EPR measurements.—X-Band (~9.7 GHz) EPR spectra were recorded as the first derivative of absorption, at 298 K, on a Bruker ESP 300E EPR spectrometer with 100 kHz field modulation. The microwave frequency was generated with a Bruker 04 ER generator and measured with a Racal-Dana frequency meter. The magnetic field was measured with a Bruker NMR-probe gaussmeter.

Spectrophotometric measurements.—The kinetics measurements were made at 350 nm, by monitoring the absorbance changes on a Jasco V530 spectrophotometer with fully thermostatted cell compartments. Reactant solutions were previously thermostatted and transferred into a cell of 1 cm path-length immediately after mixing, and disappearance of Cr^{VI} was monitored until at least 80% conversion. Experiments were performed at 30 °C unless otherwise stated. In most experiments the concentration of Cr^{VI} was kept constant at 8×10^{-4} M, while the sugar concentration was varied from 0.05 to 0.7 M. The first-order dependence of the rate upon $[Cr^{VI}]$ was verified for both anomers. The pseudo-first-order rate constants were calculated at various $[Cr^{VI}]_0$, but at constant temperature, $[Glc]_0$ and [PPTS]. As expected on the basis of a $-d(\ln[Cr^{VI}])/dt = k_{obs}$ rate law where $k_{obs} = f([Glc][PPTS])$, k_{obs} was found to be essentially constant with increasing $[Cr^{VI}]_0$. During the reaction course, the band at 350 nm decreased in intensity while a new band at 618 nm grew in (Fig. 1). At the end of the reaction, two absorbance bands ascribed to Cr^{III} d–d transitions at $\lambda_{max} = 445$ nm ($\varepsilon = 28.8\ M^{-1}\ cm^{-1}$) and 618 nm ($\varepsilon = 30.4\ M^{-1}\ cm^{-1}$) were observed for both anomers. These spectral maxima and intensities are in close agreement with those observed for Me_2SO solutions of the Cr^{3+} ion.

Product analysis.—Qualitative identification of gluconic acid as the reaction product was carried out by HPLC. The chromatograms were obtained on a KNK-500 A chromatograph equipped with a 7125 HPLC pump and a 115 Gilson UV–Vis detector. The separation was carried out on an S5 amine resin Spherisorb HPLC column using a 73:27 mixture of acetonitrile–0.1 M buffer phosphate (pH 6.4) as eluent, and a flow rate of 1.0 mL min^{-1} at $T = 30$ °C. For the reactant concentrations used in the kinetic measurements performed in Me_2SO (60 times excess of Glc over Cr^{VI} and [PPTS] = 0.02 M), gluconic acid (gluconate) was the only reaction product detected by this technique and it was identified

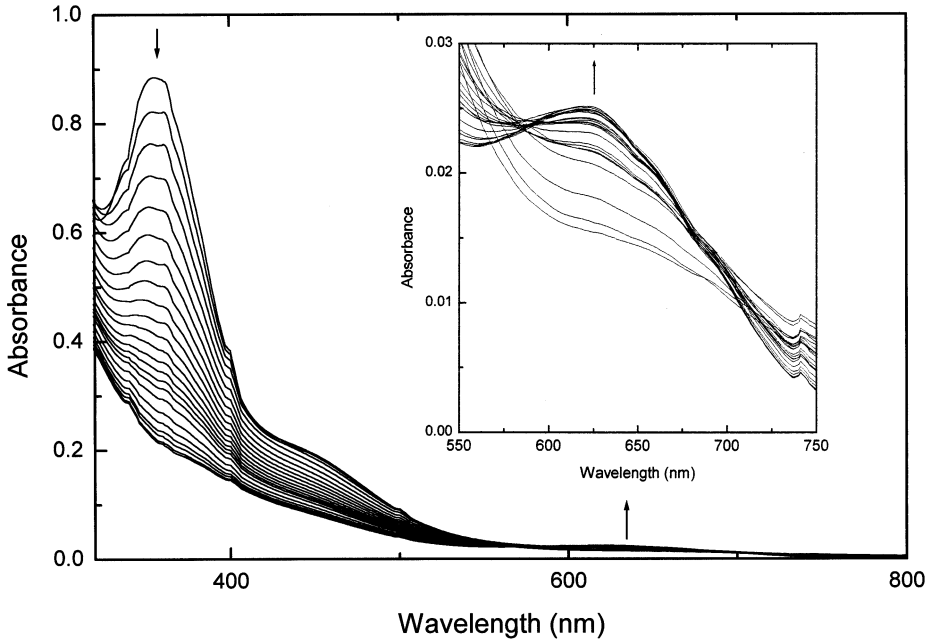

Fig. 1. Time evolution of the UV–Vis spectrum of a mixture of α-Glc (0.555 M) and Cr^{VI} (8×10^{-4} M). [PPTS] = 0.02 M; $T = 30$ °C, over a period of ~60 min.

by comparison against an authentic sample. Co-chromatography of the reaction mixture and gluconate results in the increase of the peaks of the reaction product appearing at $t = 6'05''$ and $7'40''$, which correspond to the open acid and the 1,4-lactone forms of gluconate. Neither glucuronic acid nor arabinonic acid was observed.

3. Results and discussion

Stability of reactants.—The Cr^{VI} stability in Me_2SO and Me_2SO–PPTS solutions was checked by UV–Vis spectroscopy. In Me_2SO, the spectrum of Cr^{VI} shows a band at 350 nm ($\varepsilon = 1314\ M^{-1}\ cm^{-1}$) and a shoulder at 450 nm ($\varepsilon = 175\ M^{-1}\ cm^{-1}$). In 0.02 M PPTS, the molar absorptivity coefficient of the band at 350 nm decreases to 938 $M^{-1}\ cm^{-1}$. UV–Vis spectra registered at different times after the preparation of the solutions in 0.02 M PPTS in Me_2SO showed identical λ_{max} and molar absorptivity coefficients as freshly prepared solutions. The stability of Glc in Me_2SO and Me_2SO–PPTS solutions was checked by HPLC. Chromatograms registered at different times after the preparation of the solutions were identical to those of the freshly prepared Glc solution.

Rate studies.—The mutarotation rate constants were measured by monitoring the optical rotation changes on a Jena polarimeter with thermostatted 20 cm tubes using the sodium D line. Reactant solutions were previously thermostatted and transferred into the cell immediately after mixing. Experiments were performed at 25 °C. The mutarotation of Glc obeys first-order kinetics under conditions investigated and rate constants were determined from the slope of plots of $\log(r_t - r_\infty)$ versus time [33]. The calculated rate constants $k = k_\alpha + k_\beta$ for various acid conditions are summarized in Table 1. In multiple measurements, the reproducibility of the rate constants is better than 5%.

Table 1
Values of rate constants ($k_\alpha + k_\beta$) for the mutarotation of α-Glc↔β-Glc in aqueous $HClO_4$ and Me_2SO–PPTS media [a]

	$10^4\ (k_\alpha + k_\beta)\ (s^{-1})$
0.036 M PPTS (Me_2SO) [b]	0.27(1)
0.08 M $HClO_4$ (H_2O) [c]	7.4(4)
0.1 M $HClO_4$ (H_2O) [c]	9.4(1)
0.2 M $HClO_4$ (H_2O) [c]	19.5(1)

[a] $T = 25$ °C.
[b] [Glc] = 0.52 M.
[c] [Glc] = 0.278 M.

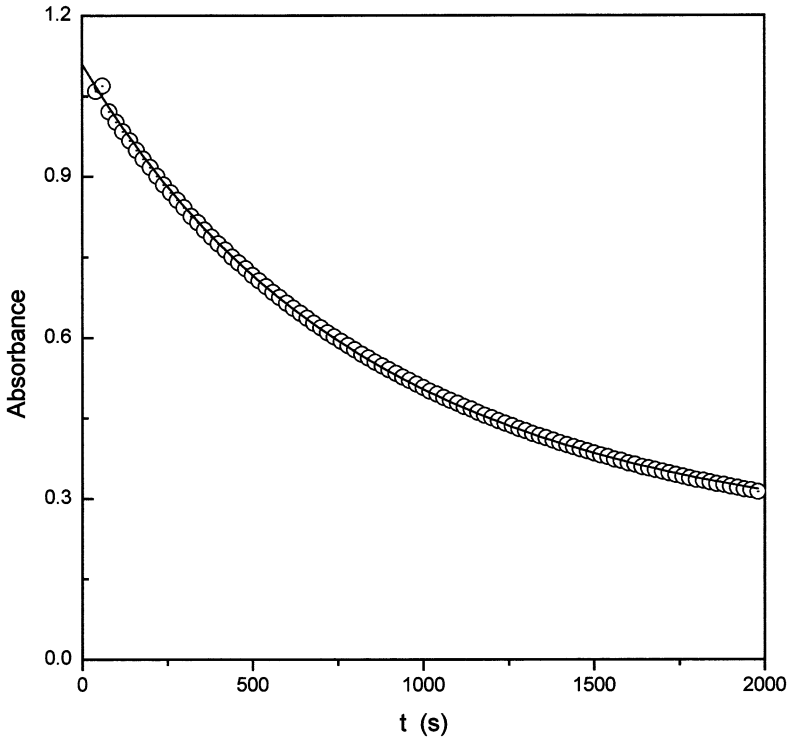

Fig. 2. Absorbance vs. time curve for the chromic oxidation of β-Glc, $[Cr^{VI}] = 8 \times 10^{-4}$ M, [β-Glc] = 0.555 M, [PPTS] = 0.02 M, $T = 30$ °C at $\lambda = 350$ nm. (⊙) Experimental, (—) calculated.

The absorbance versus time curves at 350 nm for the chromic oxidation of α-Glc and β-Glc exhibit a decrease of absorbance, which cannot be described by a single-exponential decay. At this wavelength, kinetic traces show an initial deviation from first-order decay over short time periods, which could be adequately described by the following set of consecutive first-order reactions:

$$Glc + Cr^{VI} \overset{slow}{\rightarrow} gluconate + Cr^{IV} \quad (1)$$

$$Glc + Cr^{IV} \rightarrow Glc^{\bullet} + Cr^{III} \quad (2)$$

$$Glc^{\bullet} + Cr^{VI} \rightarrow gluconate + Cr^{V} \quad (3)$$

$$Glc + Cr^{V} \overset{slow}{\rightarrow} gluconate + Cr^{III} \quad (4)$$

If intermediate Cr^{V} species and the final Cr^{III} species superimpose Cr^{VI} absorbance, the absorbance at 350 nm, at any time during the reaction, is given by:

$$Abs^{350} = \{\varepsilon^{VI}[Cr^{VI}] + \varepsilon^{V}[Cr^{V}] + \varepsilon^{III}[Cr^{III}]\}l \quad (5)$$

Combining Eq. (5) with rate expressions [34] derived from Eqs. (1)–(4), yields:

$$Abs^{350} = Abs_0 e^{-k_6 t} + k_6 \varepsilon^{V}[Cr^{VI}]_0 (e^{-k_5 t} - e^{-2k_6 t})/(2k_6 - k_5) + Abs_{\infty}\{1 + [(k_5 - k_6)e^{-2k_6 t} - k_6 e^{-k_5 t}] \times /(2k_6 - k_5)\} \quad (6)$$

The molar absorptivity of Cr^{V} at 350 nm (ε^{V}) was assumed to be the same as for the complex $[Cr^{V}(O)(ehba)_2]^-$ in Me_2SO (1390 M^{-1} cm^{-1}). Parameters k_6 and k_5 refer to the rate of disappearance of Cr^{VI} and Cr^{V}, respectively, and were evaluated from a nonlinear iterative computer fit of Eq. (6). Fig. 2 shows a typical curve for one run at 350 nm and the curve fit according to Eq. (6). The calculated kinetic parameters, k_6 and k_5, for various concentrations of Glc in 0.02 M PPTS, are summarized in Table 2. In multiple measurements, the reproducibility of the two rate constants is better than 10%.

Cr^{VI} oxidation of α-Glc and β-Glc.—The oxidation of D-glucose by Cr^{VI} in acid aqueous solution yields gluconic acid and Cr^{3+} as final products when an excess of sugar over Cr^{VI} is used. In 0.75 M $HClO_4$, k_6 values are in the range $1.7–7.3 \times 10^{-4}$ s^{-1} (Glc to Cr^{VI} ratios of 25–250:1) at 33 °C, and the redox reaction rate increases with increasing H^+ concentration [27]. The mutarotation rates in $HClO_4$ (Table 1) are higher than the

corresponding redox rates at the same H^+ concentration. Thus, it is not possible to measure the redox reaction rates of the individual anomers because they equilibrate faster than they react with Cr^{VI}. We found that in Me_2SO, the redox rates become faster than the mutarotation ones in the presence of PPTS as the proton source (Table 2).

Table 2
Observed pseudo-first-order rate constants (k_6 and k_5) for the chromic oxidation of α- and β-D-glucose [a]

[Glc] (M)	k_6 (s^{-1}) and k_5 (s^{-1})			
	α-Glc		β-Glc	
	10^4k_6	10^4k_5	10^4k_6	10^4k_5
0.0278	3.88(1)	0.83(1)		
0.0555	7.2(3)	2.52(4)	4.64(4)	1.11(5)
0.1388	8.57(7)	4.84(6)	6.79(8)	4.30(9)
0.2777	8.84(9)	8.5(3)	8.98(4)	11.1(3)
0.4166	8.8(4)	11.5(2)	8.50(8)	13.7(1)
0.5555	9.87(1)	11.2(1)	11.7(2)	17.5((1)
0.6944	9.20(1)	11.3(1)	11.2(3)	22.7(2)

[a] $T = 30$ °C; $[Cr^{VI}]_0 = 8.0 \times 10^{-4}$ M; [PPTS] $= 2.0 \times 10^{-2}$ M.

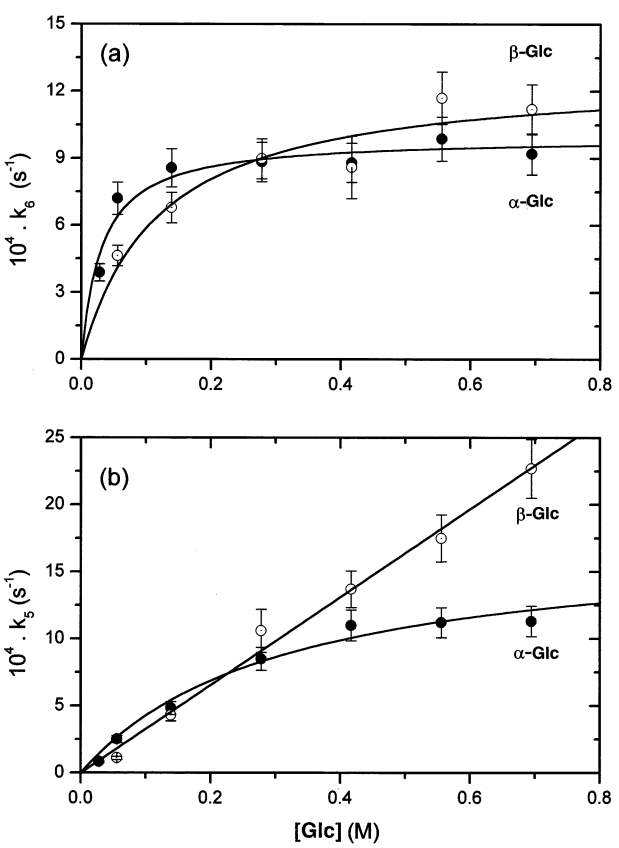

Fig. 3. Effect of [Glc] on (a) k_6 and (b) k_5, at 30 °C and $[Cr^{VI}] = 8 \times 10^{-4}$ M, [PPTS] $= 0.02$ M.

Table 3
Kinetic parameters independent of the [Glc] [a]

	α-Glc	β-Glc
k (s^{-1}) [b]	$1.0(4) \times 10^{-3}$	$1.3(1) \times 10^{-3}$
K (M^{-1}) [b]	35(5)	8(2)
k' (s^{-1}) [c]	$1.8(2) \times 10^{-3}$	
K' (M^{-1}) [c]	2.9(6)	
k'' (M^{-1} s^{-1}) [d]		$3.3(1) \times 10^{-3}$

[a] $T = 30$ °C; $[Cr^{VI}]_0 = 8.0 \times 10^{-4}$ M; [PPTS] $= 2.0 \times 10^{-2}$ M.
[b] Calculated from Eq. (7).
[c] Calculated from Eq. (10).
[d] Calculated from Eq. (11).

For the two anomers, in 0.02 M PPTS, plots of k_6 versus [α-Glc] or [β-Glc] show kinetic profiles yielding saturation curves (Fig. 3). The effect of the Glc concentration on k_6 is described by:

$$k_6 = kK[\mathrm{Glc}]/(1 + K[\mathrm{Glc}]) \quad (7)$$

from which values of k and K were determined (Table 3). Thus, the experimental rate law is expressed by:

$$-\mathrm{d}[Cr^{VI}]/\mathrm{d}t = k_6[Cr^{VI}]_T = kK[\mathrm{Glc}][Cr^{VI}]_T/(1 + K[\mathrm{Glc}]) \quad (8)$$

where $[Cr^{VI}]_T$ represents the total Cr^{VI} concentration. This kinetic law indicates that any of the anomers form an intermediate complex precursor of the redox steps as illustrated in Eq. (9):

$$Cr^{VI} + \mathrm{Glc} \overset{K}{\rightleftharpoons} [Cr^{VI}(O)_2(\mathrm{GlcH}_{-2})(Me_2SO)_2] \overset{k}{\rightarrow} \mathrm{gluconate} + Cr^{VI} \quad (9)$$

It is known that the chromic oxidations are preceded by the formation of a five-membered chelate chromate (the five-membered chromate esters are the most favorably formed) within which the electron-transfer process takes place [35,36]. In our case, this intermediate complex may be interpreted as a monochelate [14] with Glc acting as a bidentate ligand bound to Cr^{VI} at the 1,2 (or 2,3 or 3,4)-diolate moiety to yield the species $[Cr(O)_2(\mathrm{GlcH}_{-2})(Me_2SO)_2]$. These three linkage isomers might be formed by coordination of the sugar with Cr^{VI} via any pair of vicinal hydroxyl groups. However, considering that

only the hemiacetalic function is oxidized, it seems reasonable to think that the complex with the anomeric hydroxyl group bound to Cr^{VI} should be the precursor of the slow redox steps. Thus, K in the kinetic law refers to the formation of all the three isomers, and k should refer to the electron-transfer step from the total complex $[Cr(O)_2(GlcH_{-2})(Me_2SO)_2]$. It is also known that a *cis*-diolate binds hypervalent chromium stronger than a *trans*-diolate and the hemiacetalic oxygen atom coordinates Cr^{VI} stronger than the carbinolic oxygen atoms [37]. Calculated K values for α-Glc are 4.4-times higher than for β-Glc, a difference which account for the stronger chelation of the *cis*-1,2-diolate moiety in the α anomer. In contrast, the redox steps are faster for the β anomer than the α anomer.

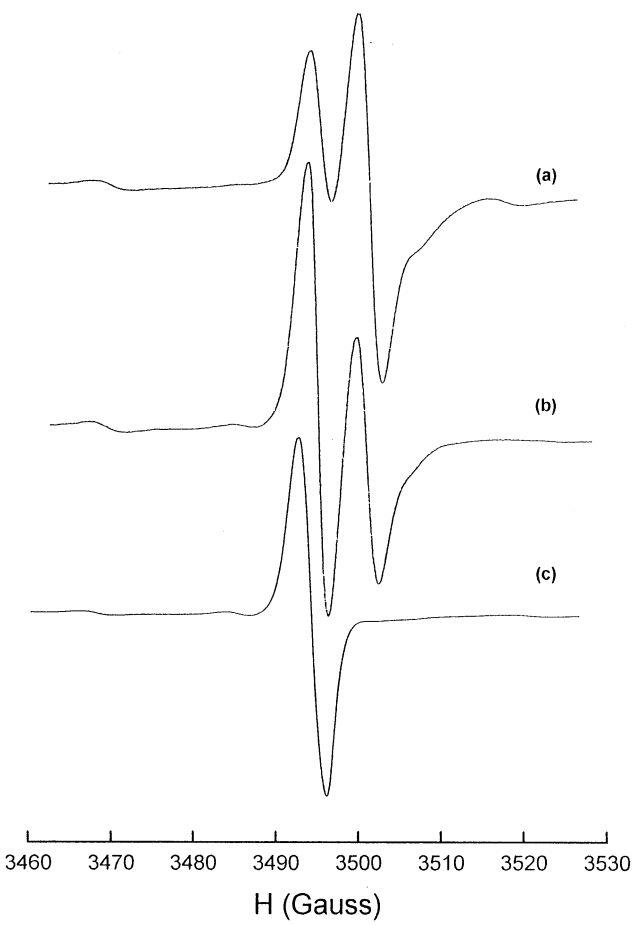

Fig. 4. X-band EPR signal of a mixture of α-Glc (0.555 M) and Cr^{VI} (0.01 M) in 0.02 M PPTS–Me_2SO and $T = 25$ °C, modulation amplitude = 0.408 G, center field = 3500 G; frequency = 9.6947 GHz. (a) 3 min; (b) 2 h; (c) 2 days, after the beginning of the reaction.

Cr^V oxidation of α-Glc and β-Glc.—The observation of Cr^V in the oxidation of Glc by Cr^{VI} is explained as follows. Cr^{IV} formed in the slow redox step (Eq. (1)) reacts with excess Glc to yield Cr^{III} and the sugar$^\bullet$ radical in a fast step (Eq. (2)). The formation of a sugar radical in the reaction of Cr^{VI} with monosaccharides has been previously demonstrated [26,27]. The rapid reaction of the radical with Cr^{VI} yields Cr^V, which further oxidizes Glc to yield the final redox products (Eqs. (3) and (4)).

Under the conditions used in the kinetic measurements, α-Glc and β-Glc are oxidized at a comparable rate by Cr^{VI} and Cr^V (Table 2). For the α anomer, the effect of the [α-Glc] on k_5 (Fig. 3) is described by Eq. (10):

$$k_5 = k'K'[\alpha\text{-Glc}]/(1 + K'[\alpha\text{-Glc}]) \quad (10)$$

Values of k' and K' (Table 3) reveal that the constant for the formation of the intermediate Cr^V complex is higher than the redox rate, and the intramolecular electron-transfer process within this Cr^V complex is twice as fast as for the α-Glc–Cr^{VI} intermediate complex. In the case of β-Glc, k_5 varies linearly with [β-Glc] (Fig. 3), probably because the intermediate Cr^V species is formed slower than it reacts and simple second-order kinetics are observed:

$$k_5 = k''[\beta\text{-Glc}] \quad (11)$$

Again, k'' is twice as fast as the electron-transfer within the β-Glc–Cr^{VI} complex.

Structure of intermediate Cr^V species.—In the PPTS–Me_2SO mixtures used in the kinetics measurements, but with a higher initial [Cr^{VI}] — required for the detection of the EPR signal — the reaction of Cr^{VI} with excess α-Glc generates three EPR signals at $g_1 = 1.9820$, $g_2 = 1.9785$ and $g_3 = 1.9756$ (Fig. 4). The signals are broad (with a 3-5 G line width) and prevent the resolution of the proton superhyperfine (shf) coupling. The g_{iso} values are informative on the Cr^V coordination number and the ligand bound to Cr^V [38], and are relatively insensitive to the nature of the solvent [39]. The observed g_{iso} values are in the range of those expected for five-coordinate oxochromate(V) complexes and they correspond to different linkage isomers of the bis-

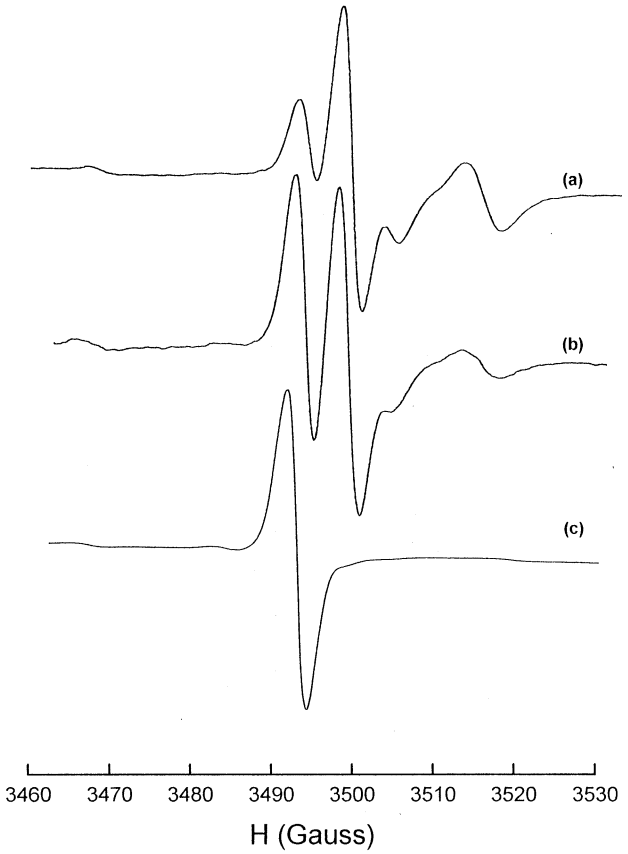

Fig. 5. X-band EPR signal of a mixture of β-Glc (0.555 M) and Cr^{VI} (0.01 M) in 0.02 M PPTS–Me_2SO and $T = 25$ °C, modulation amplitude = 0.408 G, center field = 3500 G; frequency = 9.6945 GHz. (a) 6 min; (b) 80 min; (c) 2 days, after the beginning of the reaction.

chelate $[Cr^{V}(O)(GlcH_{-2})_2]^{-}$ formed with two Glc molecules bound to Cr^{V} via the 1,2(2,3- and/or 3,4-)-diolate moieties [38]. The relative intensity of the three Cr^{V} intermediate species varies with time (Fig. 4(b)) and after a few hours the species giving rise to the signal at g_1 is the major one and remains in solution for several days (Fig. 4(c)). For this signal (g_1), it is possible to observe the four weak ^{53}Cr (9.55% abundance, $I = 3/2$) hyperfine peaks at 15.9×10^{-4} cm^{-1} spacing, typical of five-coordinate oxochromate(V) complexes [38,40].

In the reaction of Cr^{VI} with β-Glc, the EPR spectrum consists of four signals at $g_1 = 1.9820$, $g = 1.9789$, $g_3 = 1.9767$ and $g_4 = 1.9700$. Again, these signals evolve differently with time and the species at g_1 accumulates in the reaction mixture while the other species decrease but with different rates (Fig. 5). Signals at g_{1-3} have values typical of five-coordinate oxochromate(V) and the $A_{iso} = 15.8 \times 10^{-4}$ cm^{-1} observed for the remaining Cr^{V} signal (g_1) confirms the assignation. However, the g_4 value is significantly lower than the values observed for the five-coordinate oxochromate(V) complexes and, since the g values of the Cr^{V} species are very sensitive to coordination [38], it may be assigned to a six-coordinate oxochromate(V) complex $[Cr^{V}(O)(GlcH_{-2})(Me_2SO)_3]^{+}$, with only one Glc acting as a bidentate ligand via any pair of vicinal alcoholate groups. This six-coordinate species is not observed in the reaction of α-Glc with Cr^{VI}. Interestingly, under conditions used in the kinetic measurements (PPTS:Cr^{VI} ratios higher than used in the EPR measurements), the Cr^{VI} is totally reduced to Cr^{III} (no Cr^{V} is observed after the total Cr^{VI} consumption). However, in the experiments performed under the EPR conditions (2:1 PPTS:Cr^{VI} ratio), 2 days after the beginning of the reaction, Cr^{III} is not formed in a measurable quantity. The EPR results provide us with two interesting points of evidence. The first is that the electron-transfer reaction within the $[Cr^{V}(O)(GlcH_{-2})_2]^{-}$ intermediate complexes requires protons to take place. The second is that PPTS favors the formation of the six-coordinate Cr^{V} species $[Cr^{V}(O)(GlcH_{-2})(Me_2SO)_3]^{+}$ and that this complex disappears when PPTS is consumed. In previous work performed in water, we had observed that the six-coordinate complex is only detected when high $[HClO_4]$ is used, but this species disappears and the five-coordinate Cr^{V} species stabilize at higher pH. Now we have additional information on this species: it is observed only when the β anomer is used. This means that the α anomer does not form this intermediate species, or else it forms but disappears faster than it forms and it cannot be detected. The difference may account as evidence for the binding of the *trans*-1,2-diolate moiety of the β anomer versus the *cis*-1,2-diolate moiety of the α anomer. The latter is expected to afford a bis-chelate easier than the former because of the enhanced ability of the *cis*-1,2-diolate to bind Cr^{V}.

Scheme 1 summarizes the EPR results. In the scheme, **B** represents the mixture of five-

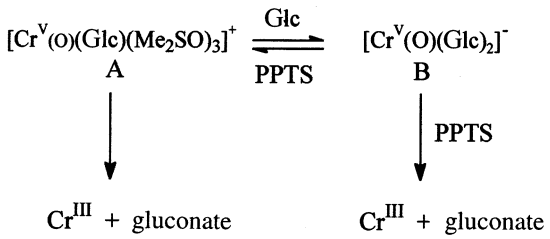

Scheme 1.

coordinate linkage isomers in equilibrium with the six-coordinate complex **A**. **A** does not require PPTS to afford the final redox products, but the intramolecular electron-transfer steps within **B** are favored by the presence of PPTS. In the absence of PPTS, the redox reaction is extremely slow and the five-coordinate Cr^V isomers (**B**) convert to the Cr^V species with the EPR signal at $g_1 = 1.9820$. In the case of the α anomer, the equilibrium **A**↔**B** is displaced towards the formation of the Cr^V bis-chelate (**B**) and, under our experimental conditions, the monochelate (**A**) is not observed.

4. Conclusions

The two anomers of Glc reduce Cr^{VI} and Cr^V at similar rates. However, these rates depend on the equilibrium constant (K) for the formation of the intermediate Glc–Cr^{VI} (and Glc–Cr^V) complex and the rate of the subsequent intramolecular electron-transfer (k), which differ from one anomer to the other. The higher $K(K')$ value for α-Glc reflects that in this anomer the 1,2-*cis*-diolate moiety favors the Cr^{VI} (Cr^V) chelation, and consequently, the activation barrier for the redox step is higher than for the intermediate chelate formed with the β anomer. Both effects compensate each other to afford the observed kinetic constants (k_5 and k_6) of the same order.

Acknowledgements

The authors thank the National Research Council of Argentina (CONICET), the Third World Academy of Sciences (TWAS), the National University of Rosario, the International Foundation for Sciences (IFS), the National Agency for Sciences Promotion and the ANTORCHAS Foundation for financial support. Thanks are also due to J.C. Gonzalez for HPLC measurements.

References

[1] C.B. Klein, in L.W. Chang (Ed.), *Toxicology of Metals*, CRC–Lewis, New York, 1996, pp. 205–220.
[2] M. Costa, *Crit. Rev. Toxicol.*, 27 (1997) 431–442.
[3] S.A. Katz, H. Salem, *The Biological and Environmental Chemistry of Chromium*, VCH, New York, 1994, pp. 65–119.
[4] D.H. Stearns, K.E. Wetterhahn, *Chem. Res. Toxicol.*, 7 (1994) 219.
[5] K.E. Wetterhahn Jannette, *J. Am. Chem. Soc.*, 104 (1982) 874–875.
[6] P. O'Brien, J. Barrett, F. Swanson, *Inorg. Chim. Acta*, 108 (1985) L19–L20.
[7] P.A. Lay, A. Levina, *J. Am. Chem. Soc.*, 120 (1998) 6704–6714.
[8] M. Ciéslak-Golonka, *Polyhedron*, 15 (1996) 3667–3689.
[9] M. Krumpolc, B.G. de Boer, J. Rocek, *J. Am. Chem. Soc.*, 100 (1978) 145–153.
[10] S.L. Brauer, K.E. Wetterhahn, *J. Am. Chem. Soc.*, 113 (1991) 3001–3007.
[11] D.M.L. Goodgame, P.B. Hayman, D.E. Hathaway, *Polyhedron*, 1 (1982) 497–499.
[12] D.M.L. Goodgame, A.M. Joy, *J. Inorg. Biochem.*, 26 (1986) 219–224.
[13] R. Codd, P. Lay, A. Levina, *Inorg. Chem.*, 36 (1997) 5440–5448.
[14] R.P. Farrell, P.A. Lay, A. Levina, I.A. Maxwell, R. Bramley, S. Brumby, J. Ji, *Inorg. Chem.*, 37 (1998) 3159–3166.
[15] R.N. Bose, B. Fonkeng, G. Barr-David, R.P. Farrell, R.J. Judd, P.A. Lay, D.F. Sangster, *J. Am. Chem. Soc.*, 118 (1996) 7139–7144.
[16] L.F. Sala, S.R. Signorella, M. Rizzotto, M.I. Frascaroli, F. Gandolfo, *Can. J. Chem.*, 70 (1992) 2046–2052.
[17] S. Signorella, S. García, L. Sala, *Polyhedron*, 11 (1992) 1391–1396.
[18] S.R. Signorella, M.I. Santoro, M.N. Mulero, L.F. Sala, *Can. J. Chem.*, 72 (1994) 398–402.
[19] M. Rizzotto, S. Signorella, M.I. Frascaroli, V. Daier, L.F. Sala, *J. Carbohydr. Chem.*, 14 (1995) 45–51.
[20] L.F. Sala, C. Palopoli, S. Signorella, *Polyhedron*, 14 (1995) 1725–1730.
[21] S. Signorella, M. Rizzotto, V. Daier, M.I. Frascaroli, C. Palopoli, D. Martino, A. Bousseksou, L.F. Sala, *J. Chem. Soc., Dalton Trans.*, (1996) 1607–1611.
[22] M. Rizzotto, M.I. Frascaroli, S. Signorella, L.F. Sala, *Polyhedron*, 15 (1996) 1517–1523.
[23] S. Signorella, S. García, L.F. Sala, *Polyhedron*, 16 (1997) 701–706.
[24] C. Palopoli, S. Signorella, L. Sala, *New J. Chem.*, 21 (1997) 343–348.
[25] S. Signorella, M. Santoro, C. Palopoli, C. Brondino, J.M. Salas-Peregrin, M. Quirós, L.F. Sala, *Polyhedron*, 17 (1998) 2739–2749.
[26] V. Daier, S. Signorella, M. Rizzotto, M.I. Frascaroli, C. Palopoli, C. Brondino, J.M. Salas-Peregrin, L.F. Sala, *Can. J. Chem.*, 77 (1999) 57–64.

[27] S. Signorella, V. Daier, S. García, R. Cargnello, J.C. González, M. Rizzotto, L.F. Sala, *Carbohydr. Res.*, 316 (1999) 14–25.
[28] S. Signorella, S. García, L.F. Sala, *J. Chem. Ed.*, 76 (1999) 405–408.
[29] C.S. Hudson, J.K. Dale, *J. Am. Chem. Soc.*, 39 (1917) 320–328.
[30] D.D. Perrin, W.L.F. Armarego, D.R. Perrin, *Purification of Laboratory Chemicals*, first ed., Pergamon Press, New York, 1966, p. 146.
[31] M. Krumpolc, J. Rocek, *Inorg. Synth.*, 20 (1980) 63–65.
[32] Fieser & Fieser's, *Reagents for Organic Synthesis*, Vol. 8, Wiley, New York, 1980, pp. 427.
[33] N.M. Ballash, E.B. Robertson, *Can. J. Chem.*, 51 (1973) 356–365.
[34] R.G. Wilkins, *The Study of Kinetics and Mechanism of Reactions of Transition Metal Complexes*, Allyn and Bacon, Boston, 1974, pp. 20–23.
[35] J.K. Beattie, G.P. Haight, in J.O. Edwards (Ed.), *Inorganic Reaction Mechanisms. Part II*, Wiley, New York, 1972.
[36] M. Mitewa, P. Bontchev, *Coord. Chem. Rev.*, 61 (1985) 241–272.
[37] P. Lay, personal communication.
[38] G. Barr-David, M. Charara, R. Codd, R. Farrel, J. Irwin, P. Lay, R. Brambley, S. Brumby, J. Ji, G. Hanson, *J. Chem. Soc., Faraday Trans.*, 91 (1996) 1207–1216.
[39] R. Brambley, J. Ji, R.J. Judd, P. Lay, *Inorg. Chem.*, 29 (1990) 3089–3094.
[40] R. Farrel, R. Judd, P. Lay, *Inorg. Chem.*, 28 (1989) 3401–3403.